Journal of Neuroscience Methods 200 (2011) 106–112

Contents lists available at ScienceDirect

Journal of Neuroscience Methods

journal homepage: www.elsevier.com/locate/jneumeth

Long-term vascular access ports as a means of sedative administration in a rodent fMRI survival model

Patrick C. Hettinger[a], Rupeng Li[b], Ji-Geng Yan[a], Hani S. Matloub[a], Younghoon R. Cho[b], Christopher P. Pawela[a,b], Daniel B. Rowe[b,c], James S. Hyde[b,*]

[a] Department of Plastic Surgery, 8700 Watertown Plank Road, Medical College of Wisconsin, Milwaukee, WI 53226, USA
[b] Department of Biophysics, 8701 Watertown Plank Road, Medical College of Wisconsin, Milwaukee, WI 53226, USA
[c] Department of Mathematics, Statistics, and Computer Science, Marquette University, 313 Cudahy Hall, 1313 West Wisconsin Avenue, Milwaukee, WI 53233, USA

ARTICLE INFO

Article history:
Received 21 May 2010
Received in revised form 2 May 2011
Accepted 18 June 2011

Keywords:
Rat fMRI
Rat fcMRI
Peripheral nerve
Vascular access port
fMRI survival study

ABSTRACT

The purpose of this study is to develop a rodent functional magnetic resonance imaging (fMRI) survival model with the use of heparin-coated vascular access devices. Such a model would ease the administration of sedative agents, reduce the number of animals required in survival experiments and eliminate animal-to-animal variability seen in previous designs. Seven male Sprague-Dawley rats underwent surgical placement of an MRI-compatible vascular access port, followed by implantable electrode placement on the right median nerve. Functional MRI during nerve stimulation and resting-state functional connectivity MRI (fcMRI) were performed at times 0, 2, 4, 8 and 12 weeks postoperatively using a 9.4 T scanner. Anesthesia was maintained using intravenous dexmedetomidine and reversed using atipamezole. There were no fatalities or infectious complications during this study. All vascular access ports remained patent. Blood oxygen level dependent (BOLD) activation by electrical stimulation of the median nerve using implanted electrodes was seen within the forelimb sensory region (S1FL) for all animals at all time points. The number of activated voxels decreased at time points 4 and 8 weeks, returning to a normal level at 12 weeks, which is attributed to scar tissue formation and resolution around the embedded electrode. The applications of this experiment extend far beyond the scope of peripheral nerve experimentation. These vascular access ports can be applied to any survival MRI study requiring repeated medication administration, intravenous contrast, or blood sampling.

1. Introduction

Since its initial description in 1990 (Ogawa et al., 1990) blood oxygen level dependent (BOLD) fMRI has provided a reliable non-invasive method for indirectly studying cerebral blood flow and neuronal activity. More recently, BOLD fMRI and fcMRI have been applied to the study of brain plasticity following nerve injury (Lundborg, 2000; Pawela et al., 2009a). Because of the homology existing between the human and rat upper extremity (Bertelli et al., 1992, 1995), the rat forelimb has served as an excellent model for human upper extremity peripheral nerve injury (Parkins et al., 2009). As fMRI and fcMRI technology continue to grow, the development of long-term rodent survival models of nerve injury has become a major focus. One adjunct to any long-term survival study is a robust method for providing intravenous access. Such access allows repeated medication administration and repeated blood sampling, if necessary. While the use of vascular access devices is not novel, there is little documentation of their use in the MRI literature. In this paper, we describe our technique for maintaining vascular access in a rodent fMRI survival study using an MRI-compatible vascular access port.

Vascular access devices have been a mainstay in animal research for decades. While successful use can be regularly achieved in large animals, smaller access devices have shown only variable success in rodents. Although earlier techniques described in the 1950s and 1960s were pivotal for the development of long-term access, many of them externalized the intravenous catheter, requiring methods to prevent catheter tampering (Cox and Beazley, 1975; Dalton et al., 1969; Edmonds and Thompson, 1970; Kleinman et al., 1975; Mendelsohn, 1962). This led to the development of multiple restraining methods along with devices designed for rotational movement (Eve and Robinson, 1963; Lemmel and Good, 1971; Rose and Nelson, 1955; Wittgenstein and Rowe, 1965). Despite modest success with these cumbersome apparatuses, improvements in sur-

Abbreviations: AFNI, analysis of functional neuroimaging; BOLD, blood oxygen level dependent; EPI, echo-planar imaging; S1FL, forelimb sensory region; fMRI, functional magnetic resonance imaging; fcMRI, functional connectivity magnetic resonance imaging; RARE, rapid acquisition with relaxation enhancement.

* Corresponding author. Tel.: +1 414 456 4005; fax: +1 414 456 6512.
E-mail address: jshyde@mcw.edu (J.S. Hyde).

0165-0270/$ – see front matter © 2011 Elsevier B.V. All rights reserved.
doi:10.1016/j.jneumeth.2011.06.018

gical technique, perioperative care, anesthesia and device-design have led to more widespread use of vascular access ports in many fields.

In the 1960s, Weeks and Davis reported on the use of indwelling catheters placed within the internal jugular vein. The group concluded that the catheter tip needed to be placed within the right atrium of the heart in order to avoid occlusion. In 1980, Kaufman directed a silastic catheter through the femoral vein to the inferior vena cava for long-term venous access. Kaufman (1980) used the femoral vein as opposed to the internal jugular vein based on previous reports of catheter occlusion. As a result of the increased flow in the femoral/inferior vena cava system, more reliable patency was established (Burvin et al., 1998; De Jong et al., 2001; Kaufman, 1980; Koeslag et al., 1984; Pages et al., 1993). In a comprehensive catheter study in 2005, Yang et al. (2005) showed patency in 100% of 3 French (Fr) catheters 9 weeks after placement in the rat femoral vein. As surgical techniques improved, so too did device design. Since the late 1990s, focus on port and catheter technology has resulted in a variety of biocompatible materials, along with multiple antithrombotic and anti-inflammatory medicated coatings (Nolan and Klein, 2002).

In rodent fMRI, the ideal survival study allows the same animal to be followed over time, with imaging obtained at specific time points. In order to maintain appropriate levels of sedation while scanning, intravenous sedatives that do not affect cerebral BOLD signal are required (Pawela et al., 2009a). Previous fMRI rodent models of nerve injury and repair required large numbers of animals to generate the statistical power necessary to make scientifically valid conclusions (Parkins et al., 2009). In these studies, all animals would undergo a nerve operation, after which groups of animals would be randomly assigned to undergo imaging at a specific time point. As a result of paralytic administration, tracheostomy, mechanical ventilation and invasive intravascular access, the animals would be euthanized immediately after imaging. The data would then be averaged for each time point, providing a picture of BOLD activation within the population at that time point. One of the inherent weaknesses of these designs is that the same animal is not followed over time, allowing animal-to-animal variability. In contrast, a survival model allowing the same animal to be followed would reduce the overall number of animals required in a survival experiment and eliminate the animal-to-animal variability seen in previous study designs. With this survival model, repeated-measures ANOVA can be performed. This will allow researchers to measure, test for differences in and account for subject variation.

As a result of the requirements for an fMRI survival study and data provided from previous catheter studies, we have developed a long-term vascular access model in the rat that is compatible with MRI. In this paper, we describe our methods using a Carmeda® BioActive Surface (CBAS)-coated, 3 Fr polyurethane catheter (Harvard Apparatus, Holliston, MA) placed in the femoral vein. The catheter is then attached to a plastic port (Harvard Apparatus, Holliston, MA), which is placed subcutaneously in the back. This technique advances our ability to conduct survival MRI studies in rats with minimal disruption to the rat between experiments, eliminating the stress of repeated vein puncture, which alters levels of multiple circulating hormones (Diehl et al., 2001; Joint Working Group on Refinement, 1993; Krinke, 2000).

2. Materials and methods

2.1. General sequence

All experiments were performed in compliance with federal regulations and the guidelines of our institutional animal care and use committee. Seven male Sprague-Dawley rats, weighing 150–200 g, were used in this study. All seven rats underwent surgical placement of a subcutaneous vascular access port. The details of this procedure are described below. Following a recovery period of one week, each rat underwent surgical placement of an implantable electrode on the right median nerve. Time of nerve surgery was considered 0. Each rat then underwent cerebral fcMRI followed by fMRI during direct nerve stimulation at times 0, 2, 4, 8 and 12 weeks postoperatively.

2.2. Animal preparation

Following an acclimation period of one week, seven male Sprague-Dawley rats, weighing 150–200 g, underwent vascular access port placement (Fig. 1). To obtain general anesthesia, the animal was placed in a transparent chamber, where isoflurane (1.4%; Halocarbon Laboratories, River Edge, NJ) was administered through a vaporizer. The animal was then transferred to the operating table where isoflurane was continuously administered through a nose cone. After obtaining adequate general anesthesia with lack of response to tail pinch, the right groin, flank and back were clipped with an electric razor. The areas were then prepped with povidone–iodine (Triad Disposables, Brookfield, WI). To begin the procedure, the animal was placed in a supine position and a 1.5 cm incision was made over the right groin. After dissecting the subcutaneous tissues, the femoral vessels were identified. The femoral vein was then isolated and ligated distally with a 6-0 silk tie. Proximally, a 6-0 tie was looped around the vein and the vein was placed under tension. A venotomy was then performed and the proximal end of the 3 Fr CBAS-coated catheter (model no. 724394, Harvard Apparatus, Holliston, MA) primed with heparinized saline (14 U/kg) was passed intraluminally 3 cm to the inferior vena cava. The catheter was then tied down with the remaining 6-0 silk tie.

The rat was then shifted to the left lateral decubitus position and attention was directed to the back. A 1.5 cm incision was placed longitudinally in the midline. A subcutaneous pocket was then dissected toward the right flank. A Kelly clamp was used to create a subcutaneous tunnel from the back incision to the groin incision. The distal end of the catheter was then retrieved and delivered into the back incision. The distal end was connected to the port (Harvard Apparatus, Holliston, MA), which was first primed with heparinized saline (14 U/kg). The catheter was then securely fixed to the port with the use of the provided locking sleeve. The port was accessed with a 22-gauge Huber needle (Smiths Medical, St. Paul, MN) drawn back to confirm patency and intraluminal position and then flushed with heparinized saline (14 U/kg). The port was then placed within the subcutaneous pocket previously dissected (Fig. 2). It is important to maintain slack in the catheter to allow for mobility of the port as the animal grows. Furthermore, the port itself was not fixed to the underlying fascia to allow for mobility during growth. The skin was then closed in both the back and groin incisions using interrupted 3-0 nylon suture. Following the surgical procedure, the animal was allowed to recover in an isolated cage. Once the animal was alert, no further isolation was required.

One week after vascular access port placement, all seven rats underwent surgical placement of an implantable electrode (AISI 304, Plastics1, Roanoke, VA) on the right median nerve (Fig. 3). Time of electrode placement was considered 0.

2.3. Anesthesia

To induce anesthesia at each time point, the animal was placed in a transparent holding chamber where vaporized isoflurane (1.4%) was administered. Following induction, the animal was transferred to the operating table and placed in the left lateral decu-

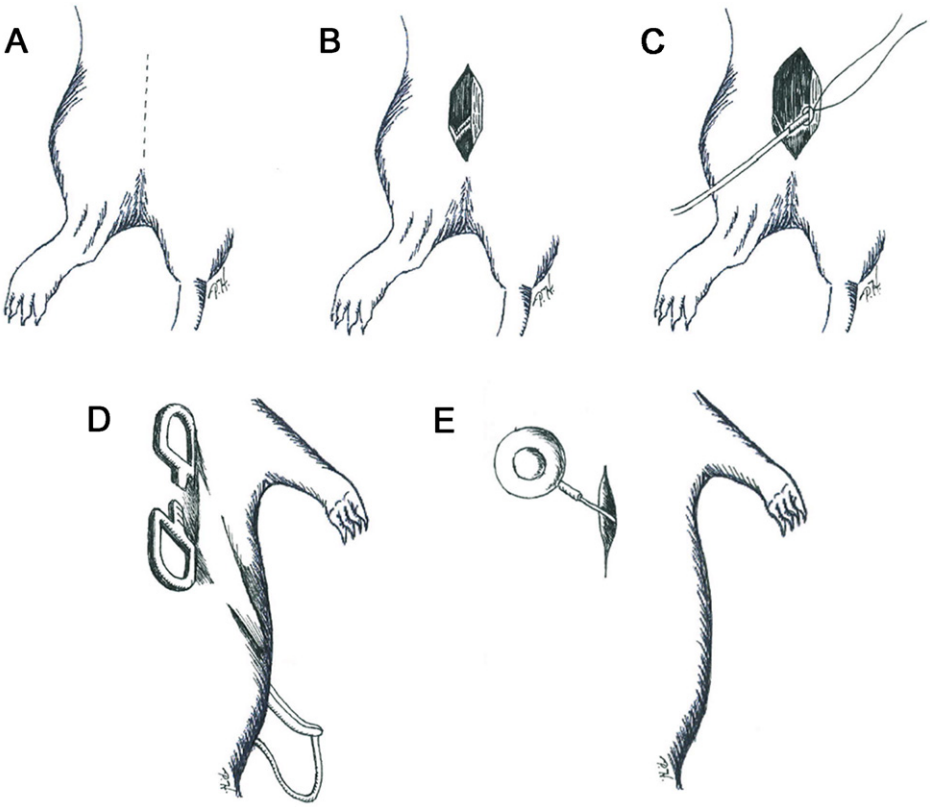

Fig. 1. Surgical technique: (A) the groin incision is marked. (B) The femoral vessels are identified. (C) The femoral vein is isolated and ligated distally. Proximally, a tie is passed around the vein. After venotomy, the catheter is passed proximally to the inferior vena cava. The catheter is then tied in place. (D) With the animal in the left lateral decubitus position, the distal end of the catheter is retrieved through a midline back incision. (E) The catheter is then fixed to the port using a provided locking sleeve.

bitus position. The port was then accessed percutaneously with a 22-gauge Huber needle using sterile technique (Fig. 4). The port was flushed with heparinized saline (14 U/kg) to confirm patency. The animal was then transferred to the 9.4 T MRI scanner. Once in the scanner, an infusion of dexmedetomidine (Orion Corp., Espoo, Finland) was started at a rate of 100 mcg/kg/h. Dexmedetomidine, the S-enantiomer of medetomidine, is an alpha-2 adrenergic agonist. Medetomidine has been shown to provide adequate depth of anesthesia while not inhibiting the BOLD signal in fMRI experimentation (Cho et al., 2007, 2008; Pawela et al., 2009a). Several minutes after the infusion was started, isoflurane was discontinued. Delaying the discontinuation of isoflurane for several minutes after starting the dexmedetomidine infusion allows the dead space of the cannula to fill and ensures intravascular circulation of dexmedetomidine. This circumvents the necessity for induction using an intravenous bolus. Rapid intravenous bolus of dexmedetomidine

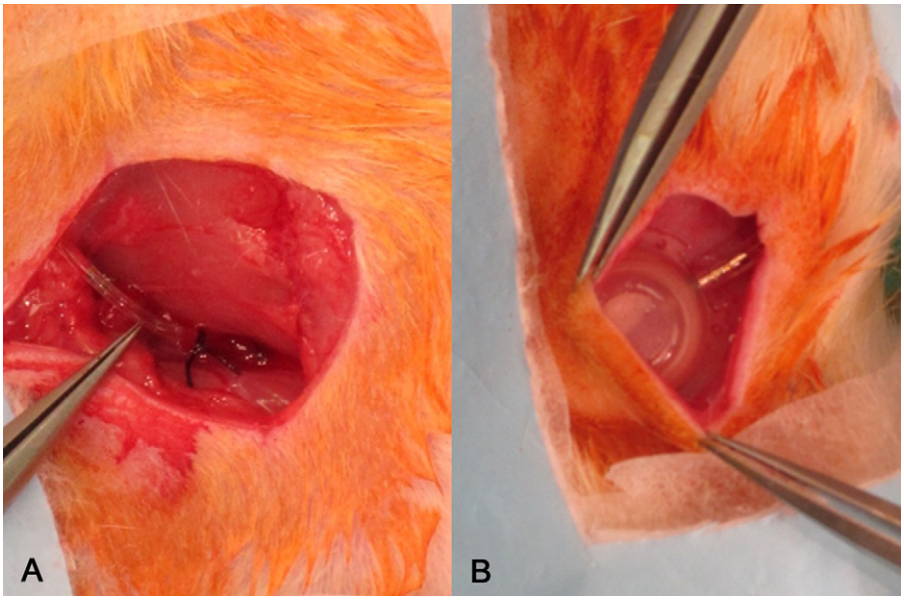

Fig. 2. Vascular access port photographs showing: (A) 3 Fr cannula within femoral vein and (B) port within subcutaneous pocket.

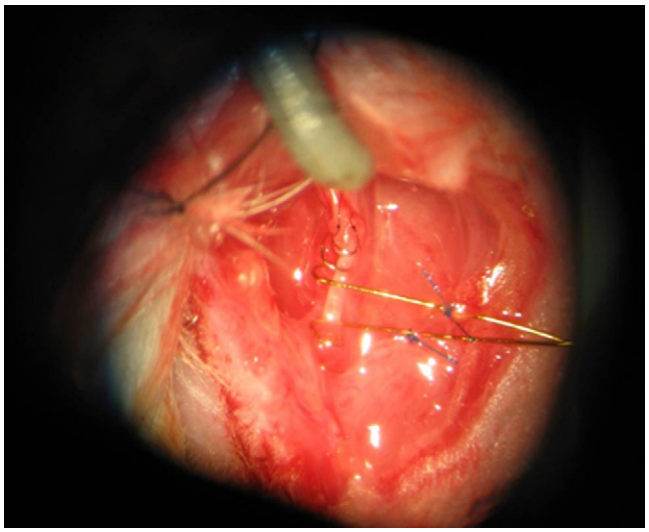

Fig. 3. Implantable electrode photograph showing subcutaneous implantable electrode placed on median nerve.

can lead to significant bradypnea, and even transient apnea, and, therefore, should be avoided.

2.4. MRI parameters and electrical stimulation methods

Methodology for fMRI using embedded electrode stimulation generally followed previous papers from this laboratory (Cho et al., 2007, 2008; Parkins et al., 2009; Pawela et al., 2009a,b). During scanning, the animal was allowed to breathe spontaneously through a nose cone with a fraction of inspired oxygen equal to 30%. Chest respiration (Model 1025, SA Instruments, Stony Brook, NY), end tidal gases (POET IQ2, Criticare Systems, Waukesha, WI) and pulse oximetry (Model 8600 V, Nonin Medical, Plymouth, MN) were continuously monitored.

The BOLD response to nerve stimulation in the primary sensory and motor regions was studied in seven animals over 12-weeks duration to determine the reproducibility of fMRI results in a longitudinal study. A Bruker AVANCE 9.4 T MRI scanner (Billerica, MA) with a 30 cm bore was used in this study. Images were acquired using a Bruker receiving surface coil (T9208) and a linear transmit coil (T10325). A rapid acquisition with relaxation enhancement (RARE) anatomic image was obtained prior to each fMRI experiment. RARE parameters were TR = 2.5 s, TE = 12.5 ms, ETL = 8, FOV = 35 mm and a 256×256 matrix. A gradient-recalled echo-planar imaging (EPI) sequence was used for fMRI and fcMRI experiments. EPI parameters were TR = 2 s, TE = 18.76 ms, FOV = 35 mm and a 96×96 matrix, with the same slice geometry as the RARE images. Ten 1-mm-thick contiguous slices were acquired, with slice 3 located directly over the anterior commissure (−0.36 mm from bregma). This slice profile allowed adequate coverage of the sensorimotor system. One-hundred-ten images were obtained during each fMRI experiment for a total acquisition time of 3 min 40 s. The fcMRI study was done before the BOLD fMRI study with no electrical stimulation applied during the scan. A square-wave electrical generator (S88, Grass Telefactor, Warrick, RI) equipped with a constant current unit (CCU, Grass Telefactor, Warrick, RI) was used for all nerve stimulations during fMRI scanning. A standard block-design stimulation protocol of 40 s rest followed by three periods of 20 s on and 40 s off was used (total of 3 min 40 s). Electrical stimulation was computer-controlled and triggered by a transistor–transistor logic pulse from the scanner. Direct nerve stimulation was performed with a current of 0.5 mA, frequency of 10 Hz and duration of 1 ms.

2.5. Anesthesia reversal

Following image acquisition, the animal was returned to the operating suite. Dexmedetomidine was then reversed using atipamezole (Orion Corp., Espoo, Finland) (100 mcg/kg given intramuscularly).

2.6. Postoperative management

To promote port patency, the vascular access device was accessed with a Huber needle biweekly and flushed with heparinized saline (14 U/kg) as previously described. All incisions were inspected and assessed for signs of infection. Furthermore, behavior (including feeding habits and ambulation) was monitored to identify any signs of postoperative complications.

2.7. Image processing

Motion correction was performed for all individual scans before any further analysis (AFNI, 3dvolreg). Datasets were detrended to eliminate linear drifts, and separate slices were aligned to the same temporal origin. The EPI scans were then registered to the anatomic images (FSL, FLIRT). For BOLD fMRI acquisitions, the registered EPI acquisitions were averaged using analysis of functional neuroimages (AFNI) software (Cox and Hyde, 1997). These averaged EPI datasets were used to create BOLD activation maps. The activation maps were created by performing an *F*-test on the time series with the block design as the only regressor (AFNI, 3dDeconvolve). Activation was determined by an *F*-test (3dDeconvolve)

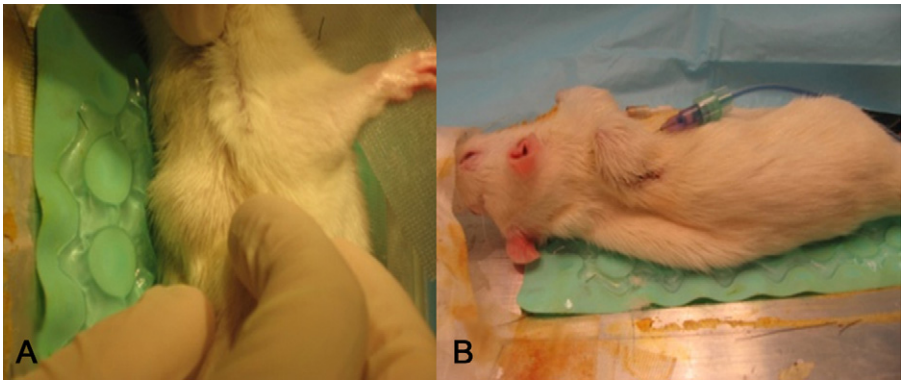

Fig. 4. Vascular port access: (A) port identified in subcutaneous pocket. (B) Port accessed percutaneously using Huber needle.

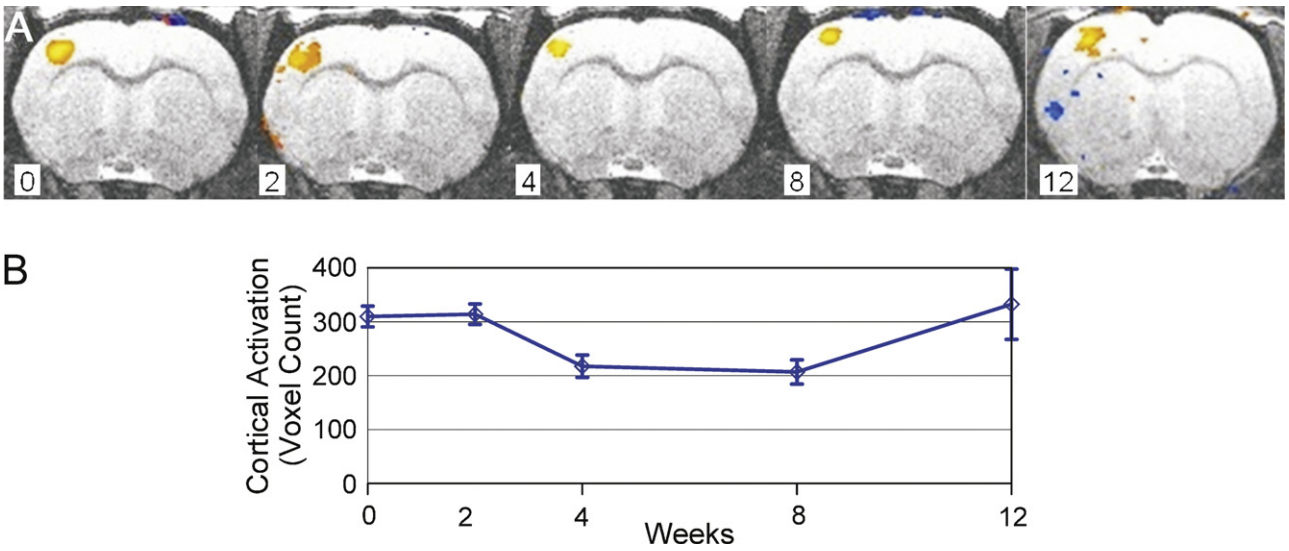

Fig. 5. (A) BOLD activation: BOLD fMRI signal seen in slice 2 (bregma + 0.64 mm) pooled across seven animals during direct median nerve stimulation at 0, 2, 4, 8 and 12 weeks postoperatively. (B) Average voxel activation was seen at time 0, 2, 4, 8 and 12 weeks.

with a *p*-value threshold of 0.005 (using AFNI). For the fcMRI study, all resting-state acquisitions were analyzed individually after registration using seed-voxel-based fcMRI analysis. The seed region was chosen from the left granular insular cortex (GI) and consisted of 25 voxels. The same seed was applied to each fcMRI scan to create a reference time course for each resting-state scan. A band-pass filter was used for all resting-state EPI acquisitions, with a low-pass filter of 0.1 Hz and a high-pass filter of 0.01 Hz on a voxel-by-voxel basis covering the entire brain (Hamming, 1983). The resting-state, voxel-wise correlation coefficient analysis was done using the reference time course of each individual scan. Results underwent fisher-*Z* transform and then were pooled based on the time point of data acquisition. The fcMRI results of each time point were generated by averaging individual fcMRI results. A histogram of voxel counts was created to demonstrate the results at a *p*-value threshold of 0.05.

3. Results

Seven animals underwent vascular access port placement along with fMRI during direct nerve stimulation at time 0, 4, 8 and 12 weeks postoperatively. Image acquisition time was 45.3 min at each time point, and the total time on the scanner approximated 70 min at each time point. During all scanning, the mean heart rate was 243 bpm (162–320 bpm), the mean respiratory rate was 87 breaths/min (43–147 breaths/min), and pulse oximetry ranged from 89 to 99%. There were no fatalities or infectious complications during this study. There were no physical findings of lymphedema or venous stasis in the right lower extremity. All vascular access ports remained patent over the 12-week time period. Patency was determined by ease of injection, adequacy of and ability to obtain general anesthesia and physical examination of the port site.

BOLD activation was seen within the forelimb sensory territory (S1FL) of the contralateral cortical hemisphere during direct nerve stimulation for all animals at all time points. Statistically significant BOLD fMRI signal activation during direct nerve stimulation is shown in Fig. 5. Fig. 5A shows the averaged voxel activation of seven animals across five time points. Fig. 5B is a graph showing the average number of activated voxels observed in the seven rats for each time point. Raw data are shown in Table 1.

The results of the fcMRI study are demonstrated in Fig. 6. Due to the highly selective seed region we used in this study (GI), a refined resting-state network can be seen within the bilateral insular cortex with great consistency across five different time points (Fig. 6A). The histogram shown in Fig. 6B further demonstrates this consistency, with the area under the curve being the sum of the voxel counts contained in the network of each time point. ANOVA was also performed using 0-week resting-state data as a reference and comparing it to the results at 2, 4, 8 and 12 weeks. There is no statistically significant change in the fcMRI network.

4. Discussion

By providing superior soft tissue contrast and detail, MRI has become a standard imaging technique for a host of central nervous system, musculoskeletal, cardiovascular and oncologic disorders. As mouse and rat models have been developed to study these and other disorders (Beaumont et al., 2009; Stuckey et al., 2008; Valable et al., 2007), rodent MRI has been used with increasing frequency in multiple fields. Furthermore, as greater emphasis has

Table 1
Voxel counts for the longitudinal study.

	Week 0	Week 2	Week 4	Week 8	Week 12
Rat 1	324	347	242	237	389
Rat 2	298	307	213	224	317
Rat 3	317	299	201	178	397
Rat 4	297	325	198	188	247
Rat 5	286	297	206	199	267
Rat 6	337	309	245	215	378
Rat 7	309	309	223	207	328
Average	309.7143	313.2857	218.2857	206.8571	331.8571
Standard deviation	19.30199	18.96312	20.79183	22.44475	65.21273

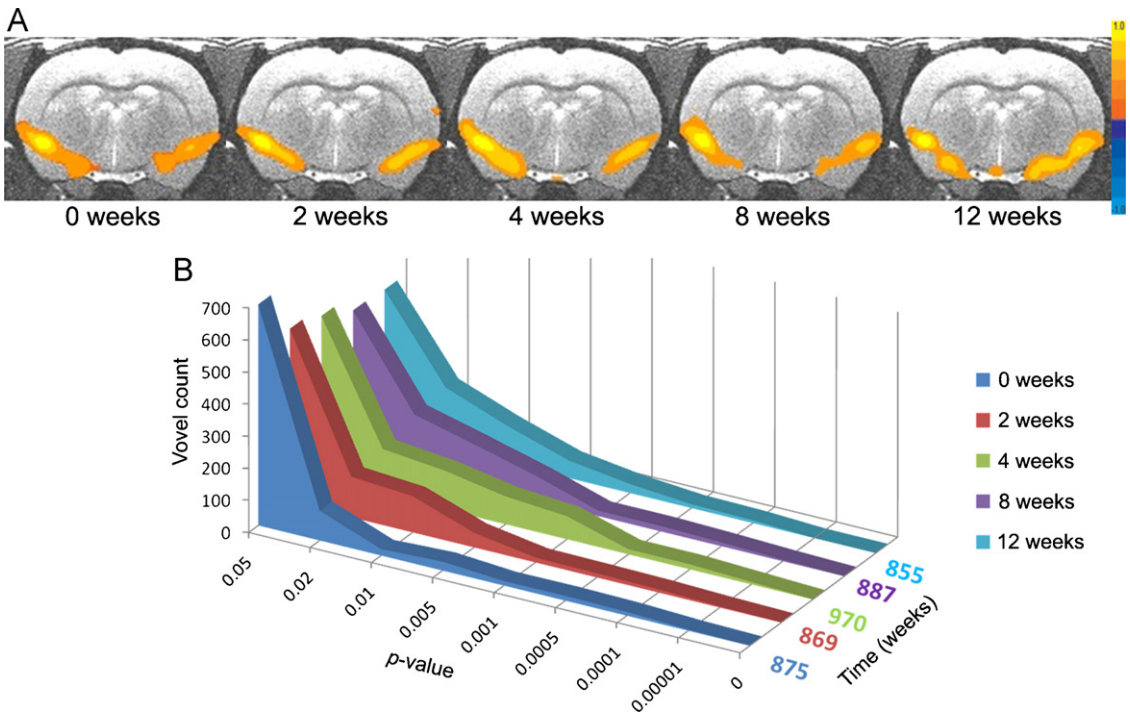

Fig. 6. Resting-state fcMRI showing an averaged insular network using a seed region from the granular insular cortex (GI). The same seed region was used across all individual animals. All results were *Z*-transformed, and a *p*-threshold of 0.05 was used. (A) Demonstrates highly consistent insular network at time points of 0, 2, 4, 8 and 12 weeks. (B) Comparison of histograms of fcMRI networks acquired at different time points. The area under the curve represents the sum of the voxel counts observed in the fcMRI network, which is demonstrated numerically on the right side of Fig. 6B. The results are highly consistent across time points.

been placed on outcomes, the need for longitudinal survival models has increased in rodent experimentation. Nearly all survival rodent studies require repeated medication administration and/or frequent blood sampling. Therefore, the maintenance of intravascular access is a helpful adjunct to any rodent survival study.

While intravenous access can be obtained from various methods, multiple studies suggest that repeated vein puncture increases animal stress and alters circulating levels of glucose, corticosteroids, prolactin, epinephrine, growth hormone, insulin and renin (Diehl et al., 2001; Joint Working Group on Refinement, 1993; Krinke, 2000). Furthermore, vein puncture is technique-dependent and often requires a period of warming for vessel dilatation. Eliminating the morbidity associated with repeat vein puncture, intravascular access devices provide for easy administration of medications and repeated blood sampling. Despite reproducible success in larger animal models, only recently has long-term patency been shown in the rodent literature (De Jong et al., 2001; Yang et al., 2005).

In the case of fMRI, the ideal survival study should allow the same animal to be imaged at multiple time points. Such a study requires sedation that does not interfere with the BOLD signal, yet permits safe animal recovery following each scan. Dexmedetomidine, an alpha-2 adrenergic agonist, has been shown to be effective in multiple BOLD fMRI studies (Cho et al., 2007, 2008; Pawela et al., 2009a). This sedative allows adequate sedation for fMRI imaging, affords the use of spontaneous breathing and has a potent reversal agent with a quick onset of action. Currently, with the use of MRI-compatible subcutaneous vascular access ports and the sedative dexmedetomidine, we have demonstrated a safe and effective model for a rodent survival fMRI study. Furthermore, with reliable intravenous access, sedative doses can easily be adjusted to accommodate longer scanning times. This protocol circumvents the morbidity associated with mechanical ventilation, eliminates animal-to-animal variability and reduces the overall number of animals required for a longitudinal study.

In this study on healthy rats, S1FL activation drop-off can be seen at time points of 4 and 8 weeks. At longer time points, the fMRI signal recovers to a relatively normal level. This progression corresponds with the natural progression of scar tissue formation following electrode placement, which peaks at about 4–8 weeks with subsequent gradual resolution. The phenomenon observed here could be the consequence of compression of the nerve trunk by developing scar tissue after electrode placement, thereby affecting the conductivity of nerve fibers via axonotmesis. Behavior tests were performed to test this hypothesis. Decreases in grip strength and in Von Frey monofilament response were observed at 4–8 weeks, consistent with this hypothesis. Behavior test results as well as fMRI results return to normal ranges at 12 weeks. These experiments support the idea that there is a coupling between scar tissue formation around peripheral nerves that have been mildly stressed by electrode placement and reduced neuronal activity.

As a control for axonotmesis, fcMRI of the insular cortex was introduced to the study. A highly consistent fcMRI insular network was acquired at the various time points after surgery. A similar insular network was reported previously using BOLD fMRI and independent component analysis (ICA) in a nonsurvival rat model (Zhang et al., 2010; Liang et al., 2011). Our study shows that this network pattern is conserved across the different time points. Due to the highly specific seed we used in this study, only the insular cortical network was demonstrated.

Based on the atlas (Paxinos and Watson, 2007), the network consists of the granular insular cortex (GI), the dysgranular insular cortex (DI), the agranular insular posterior cortex (AIP) and the piriform cortex. These areas are related to signal integration, synaptic plasticity and memory (Blair et al., 2001; Sweatt, 2001), which can also be modified by task (Kida et al., 2011). It is hypothesized that fcMRI of granular insular cortex can be used as a control in fMRI survival experiments of various kinds including cortical plasticity studies.

In this study, seven vascular access ports remained patent over a period of 12 weeks. This experiment is exciting in that long-term vascular access can be reproducibly achieved and used safely in a rodent survival MRI study. The applications of such a port extend far beyond the scope of peripheral nerve experimentation. Such access ports can be applied to any survival MRI study requiring repeated medication administration, intravenous contrast or blood sampling.

Acknowledgement

This work was supported by grant EB000215 of the National Institutes of Health.

References

Beaumont M, Lemasson B, Farion R, Segebarth C, Remy C, Barbier EL. Characterization of tumor angiogenesis in rat brain using iron-based vessel size index MRI in combination with gadolinium-based dynamic contrast-enhanced MRI. J Cereb Blood Flow Metab 2009;29:1714–26.

Bertelli JA, Mira JC, Gilbert A, Michot GA, Legagneux J. Anatomical basis of rat brachial plexus reconstruction. Surg Radiol Anat 1992;14:85–6.

Bertelli JA, Taleb M, Saadi A, Mira JC, Pecot-Dechavassine M. The rat brachial plexus and its terminal branches: an experimental model for the study of peripheral nerve regeneration. Microsurgery 1995;16:77–85.

Blair HT, Schafe GE, Bauer EP, Rodrigues SM, LeDoux JE. Synaptic plasticity in the lateral amygdala: a cellular hypothesis of fear conditioning. Learn Mem 2001;8:229–42.

Burvin R, Zloczower M, Karnieli E. Double-vein jugular/inferior vena cava clamp technique for long-term *in vivo* studies in rats. Physiol Behav 1998;63:511–5.

Cho YR, Pawela CP, Li R, Kao D, Schulte ML, Runquist ML, et al. Refining the sensory and motor ratunculus of the rat upper extremity using fMRI and direct nerve stimulation. Magn Reson Med 2007;58:901–9.

Cho YR, Jones SR, Pawela CP, Li R, Kao DS, Schulte ML, et al. Cortical brain mapping of peripheral nerves using functional magnetic resonance imaging in a rodent model. J Reconstr Microsurg 2008;24:551–7.

Cox CE, Beazley RM. Chronic venous catheterization: a technique for implanting and maintaining venous catheters in rats. J Surg Res 1975;18:607–10.

Cox RW, Hyde JS. Software tools for analysis and visualization of fMRI data. NMR Biomed 1997;10:171–8.

Dalton RG, Touraine JL, Wilson TR. A simple technique for continuous intravenous infusion in rats. J Lab Clin Med 1969;74:813–5.

De Jong WH, Timmerman A, van Raaij MT. Long-term cannulation of the vena cava of rats for blood sampling: local and systemic effects observed by histopathology after six weeks of cannulation. Lab Anim 2001;35:243.

Diehl KH, Hull R, Morton D, Pfister R, Rabemampianina Y, Smith D, et al. A good practice guide to the administration of substances and removal of blood, including routes and volumes. J Appl Toxicol 2001;21:15–23.

Edmonds CJ, Thompson BD. A method allowing intravenous infusion of unrestrained rats for several weeks. J Physiol 1970;207:41P–2P.

Eve C, Robinson SH. Apparatus for continuous long-term intravenous infusions in small animals. J Lab Clin Med 1963;62:169.

Hamming RW. Digital filters. Englewood Cliffs, NJ: Prentice Hall; 1983.

Joint Working Group on Refinement. Removal of blood from laboratory mammals and birds. Lab Anim 1993;17:1–22.

Kaufman S. Chronic, nonocclusive and maintenance-free central venous cannula in the rat. Am J Physiol 1980;239:R123–5.

Kida I, Iguchi Y, Hoshi Y. Blood oxygenation level-dependent functional magnetic resonance imaging of bilateral but asymmetrical response to gustatory stimulation in the rat insular cortex. Neuroimage 2011;56:1520–5.

Kleinman LI, Radford EP, Torelli G. Urea and inulin clearances in undisturbed, unanesthetized rats. Am J Physiol 1975;208:578.

Koeslag D, Humphreys AS, Russell JC. A technique for long-term venous cannulation in rats. J Appl Physiol 1984;57:1594–6.

Krinke GJ. The laboratory rat. 1st ed. London: Academic Press; 2000.

Lemmel EM, Good RA. Continuous long-term intravenous infusion in unrestrained mice – method. J Lab Clin Med 1971;77:1011–4.

Liang Z, King J, Zhang N. Uncovering intrinsic connectional architecture of functional networks in awake rat brain. J Neurosci 2011;31:3776–83.

Lundborg G. Brain plasticity and hand surgery: an overview. J Hand Surg [Br] 2000;25:242–52.

Mendelsohn ML. Chronic infusion of tritiated thymidine into mice with tumors. Science 1962;135:213–5.

Nolan TE, Klein HJ. Methods in vascular infusion biotechnology in research with rodents. ILAR J 2002;43:175–82.

Ogawa S, Lee TM, Nayak AS, Glynn P. Oxygenation-sensitive contrast in magnetic resonance image of rodent brain at high magnetic fields. Magn Reson Med 1990;14:68–78.

Pages T, Fernandez JA, Adan C, Gamez A, Viscor G, Palacios L. A method for sampling representative muscular venous blood during exercise in rats. Lab Anim 1993;27:171–5.

Parkins MA, Li R, Matloub HS, Yan JG, Hyde JS, Pawela CP. A peripheral nerve repair model using fMRI in rats [abstract]. Proc Intl Soc Mag Reson Med 2009;17:1680.

Pawela CP, Biswal BB, Hudetz AG, Schulte ML, Li R, Jones SR, et al. A protocol for use of medetomidine anesthesia in rats for extended studies using task-induced BOLD contrast and resting-state functional connectivity. Neuroimage 2009a;46:1137–47.

Pawela CP, Biswal BB, Hudetz AG, Li R, Jones SR, Cho YR, et al. Interhemispheric neuroplasticity following limb deafferentation detected by resting-state functional connectivity magnetic resonance imaging (fcMRI) and functional magnetic resonance imaging (fMRI). Neuroimage 2009b;49:2467–78.

Paxinos G, Watson C. The rat brain in stereotaxic coordinates. 6th ed. Amsterdam, Netherlands: Elsevier; 2007.

Rose S, Nelson JF. A continuous long-term injector. Aust J Exp Biol Med Sci 1955;33:415.

Stuckey DJ, Carr CA, Tyler DJ, Aasum E, Clarke K. Novel MRI method to detect altered left ventricular ejection and filling patterns in rodent models of disease. Magn Reson Med 2008;60:582–7.

Sweatt JD. The neuronal MAP kinase cascade: a biochemical signal integration system subserving synaptic plasticity and memory. J Neurochem 2001;76:1–10.

Valable S, Barbier EL, Bernaudin M, Roussel S, Segebarth C, Petit E, et al. *In vivo* MRI tracking of exogenous monocytes/macrophages targeting brain tumors in a rat model of glioma. Neuroimage 2007;37:S47–58.

Wittgenstein E, Rowe Jr KW. A technique for prolonged infusion of rats. Lab Anim Care 1965;15:375–8.

Yang J, Maarek JM, Holschneider DP. *In vivo* quantitative assessment of catheter patency in rats. Lab Anim 2005;39:259–68.

Zhang N, Rane P, Huang W, Liang Z, Kennedy D, Frazier JA, et al. Mapping resting state brain networks in conscious animals. J Neurosci Methods 2010;189:186–96.